

Effects of Surface Force-Constant Changes on the Atomic Mean Square Displacements in Face-Centered Cubic Crystals with a Free Surface

R. F. WALLIS

Naval Research Laboratory, Washington, D. C.

AND

B. C. CLARK AND R. HERMAN

General Motors Research Laboratories, Warren, Michigan

(Received 20 November 1967)

In a crystal with a free surface, the force constants associated with the coupling of surface atoms to their neighbors need not be the same as those associated with the coupling of interior atoms. A theoretical investigation has been made of the effect on the atomic mean square displacements of varying the force constants for surface atoms on the (110) surface of a face-centered cubic crystal. The bonds coupling atoms on such a surface to their nearest neighbors may be grouped into three classes, depending on the angle between the bond and the normal to the surface. The force constants for each of these three types of surface bonds have been varied independently, and the mean square displacements have been evaluated in the high-temperature limit of the harmonic approximation, using the nearest-neighbor central force model for crystals up to thirty layers thick. A comparison is given between the theoretical results and experimental low-energy electron diffraction data for the (110) surface of nickel.

I. INTRODUCTION

THE development of low-energy electron-diffraction techniques has provided a means of obtaining information about the mean square displacements of surface atoms.¹ MacRae² has carried out a detailed experimental investigation of the (110) surface of nickel and has found that the parallel and perpendicular mean-square-displacement components are different. Furthermore, he found that the two parallel values are not equal to each other.

In a previous paper,³ theoretical calculations have been made of the mean-square-displacement components of atoms in the (100), (110), and (111) surfaces of a nickel-crystal model with nearest-neighbor central forces. The harmonic approximation in the high-temperature limit was employed, with no change in the force constants at or near the surface. The results for the (110) surface were in good qualitative agreement with the experimental results of MacRae, but there were certain quantitative discrepancies. Specifically, the calculated mean-square-displacement components in the [110] and [001] directions were too small compared to the experimental values. A number of possible reasons for this discrepancy were discussed.³ First, there is the possibility that the assumptions involved in calculating the experimental values of the mean square displacements from the experimental data are not valid. Second, the theoretical calculations may involve too simple a model, in that it neglects longer-range interactions, anharmonicity, magnetic effects, and changes in the force constants at or near the surface. Finally, the

theoretical calculations were done on finite-sized crystals very much smaller than those used in the experiments. In the present paper, one of these possibilities, which is considered most important, is investigated theoretically, namely, that the force constants characterizing the interactions of the surface atoms may have values different from their bulk values.

II. THEORETICAL PROCEDURE

The methods employed in the present paper are basically the same as those of Ref. 3. A model of a face-

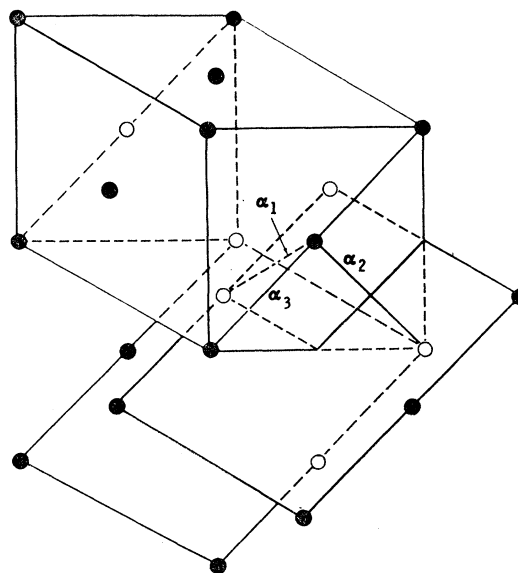


FIG. 1. Diagram of the interactions of an atom in the (110) surface. The bond α_1 makes an angle of 30° to the surface and connects a surface atom with an atom one layer removed, α_2 is perpendicular to the surface and connects a surface atom to an atom two layers removed, and α_3 is parallel to the surface. Closed circles are visible atoms.

¹ A. U. MacRae and L. H. Germer, *Phys. Rev. Letters* **8**, 489 (1962).

² A. U. MacRae, in *Proceedings of the International Conference on the Physics and Chemistry of Solid Surfaces*, Brown University, June, 1964 (unpublished); *Surface Sci.* **2**, 522 (1964).

³ B. C. Clark, R. Herman, and R. F. Wallis, *Phys. Rev.* **139**, 860 (1965).

centered cubic lattice is assumed with nearest-neighbor central forces. The free surface is taken to be parallel to a (110) plane. The nearest-neighbor interactions of a surface atom for this particular surface can be classified into three different types, as may be seen from an examination of Fig. 1. The interaction of Type 1 couples the surface atom to an atom in an adjacent (110) plane, the line of centers of the two atoms making an angle of 30° with the surface. The Type-2 interaction couples the surface atom with an atom two layers away and is normal to the surface. The Type-3 interaction couples two atoms in the surface layer and is therefore parallel to the surface. Associated with these interactions are three force constants α_1 , α_2 , and α_3 , respectively, which need not be equal for a surface atom, even though they would be equal by symmetry if the atom were infinitely far from the surface.

The positions of the atoms will be specified in terms

of three basis vectors given by

$$\boldsymbol{\tau}_1 = \frac{1}{2}(a, 0, 0), \quad (1a)$$

$$\boldsymbol{\tau}_2 = \frac{1}{2}(0, a, 0), \quad (1b)$$

$$\boldsymbol{\tau}_3 = \frac{1}{2}(0, 0, 2^{1/2}a), \quad (1c)$$

where a is the nearest-neighbor lattice spacing.

The 2 and 3 directions, which may be taken in the $[\bar{1}10]$ and $[001]$ directions, respectively, are parallel to a (110) plane, while the 1 direction, which may be taken in the $[110]$ direction, is normal to the (110) plane. The coordinates of a lattice site can then be expressed as

$$\mathbf{r}_{l,m,n} = l\boldsymbol{\tau}_1 + m\boldsymbol{\tau}_2 + n\boldsymbol{\tau}_3, \quad (2)$$

where l , m , n are either all even integers or all odd integers, taking zero to be even.

The equations of motion for a bulk atom can now be written as

$$m_0 \ddot{u}_{l,m,n} = \frac{1}{4}\alpha \left\{ -8u_{l,m,n} + \sum_{\lambda,\mu,\nu=\pm 1} u_{l+\lambda,m+\mu,n+\nu} - 8u_{l,m,n} + 4 \sum_{\lambda=\pm 2} u_{l+\lambda,m,n} + \sum_{\lambda,\mu,\nu=\pm 1} \lambda \mu v_{l+\lambda,m+\mu,n+\nu} + 2^{1/2} \sum_{\lambda,\mu,\nu=\pm 1} \lambda \nu w_{l+\lambda,m+\mu,n+\nu} \right\}, \quad (3a)$$

$$m_0 \ddot{v}_{l,m,n} = \frac{1}{4}\alpha \left\{ -8v_{l,m,n} + \sum_{\lambda,\mu,\nu=\pm 1} v_{l+\lambda,m+\mu,n+\nu} - 8v_{l,m,n} + 4 \sum_{\mu=\pm 2} v_{l,m+\mu,n} + \sum_{\lambda,\mu,\nu=\pm 1} \lambda \mu u_{l+\lambda,m+\mu,n+\nu} + 2^{1/2} \sum_{\lambda,\mu,\nu=\pm 1} \lambda \mu \nu w_{l+\lambda,m+\mu,n+\nu} \right\}, \quad (3b)$$

$$m_0 \ddot{w}_{l,m,n} = \frac{1}{4}\alpha \left\{ 2(-8w_{l,m,n} + \sum_{\lambda,\mu,\nu=\pm 1} w_{l+\lambda,m+\mu,n+\nu} + 2^{-1/2} \sum_{\lambda,\mu,\nu=\pm 1} \lambda \nu u_{l+\lambda,m+\mu,n+\nu} + 2^{-1/2} \sum_{\lambda,\mu,\nu=\pm 1} \mu \nu v_{l+\lambda,m+\mu,n+\nu}) \right\}, \quad (3c)$$

where m_0 is the atomic mass, α is the nearest-neighbor force constant, and $u_{l,m,n}$, $v_{l,m,n}$, and $w_{l,m,n}$ are the atomic-displacement components in the 1, 2, and 3 directions, respectively. The equations of motion for atoms in the surface layer, $l=0$, may be written as

$$m_0 \ddot{u}_{0,m,n} = \frac{1}{4}\alpha \left\{ \epsilon_1 [-4u_{0,m,n} + \sum_{\mu,\nu=\pm 1} (u_{1,m+\mu,n+\nu} + \mu v_{1,m+\mu,n+\nu} + 2^{1/2} \nu w_{1,m+\mu,n+\nu})] + 4\epsilon_2 (u_{2,m,n} - u_{0,m,n}) \right\}, \quad (4a)$$

$$m_0 \ddot{v}_{0,m,n} = \frac{1}{4}\alpha \left\{ \epsilon_1 [-4v_{0,m,n} + \sum_{\mu,\nu=\pm 1} (\mu u_{1,m+\mu,n+\nu} + v_{1,m+\mu,n+\nu} + 2^{1/2} \mu \nu w_{1,m+\mu,n+\nu})] + \epsilon_2 (-8v_{0,m,n} + 4 \sum_{\mu=\pm 2} v_{0,m+\mu,n}) \right\}, \quad (4b)$$

$$m_0 \ddot{w}_{0,m,n} = \frac{1}{4}\alpha \left\{ 2\epsilon_1 [-4w_{0,m,n} + \sum_{\mu,\nu=\pm 1} (2^{-1/2} \nu u_{1,m+\mu,n+\nu} + 2^{-1/2} \mu \nu v_{1,m+\mu,n+\nu} + w_{1,m+\mu,n+\nu})] \right\}, \quad (4c)$$

where

$$\epsilon_i = \alpha_i / \alpha, \quad i = 1, 2, 3. \quad (5)$$

The equations of motion for the layer next to the surface layer, $l=1$, are

$$m_0 \ddot{u}_{1,m,n} = \frac{1}{4}\alpha \left\{ \epsilon_1 [-4u_{1,m,n} + \sum_{\mu,\nu=\pm 1} (u_{0,m+\mu,n+\nu} - \mu v_{0,m+\mu,n+\nu} - 2^{1/2} \nu w_{0,m+\mu,n+\nu})] - 4u_{1,m,n} + \sum_{\mu,\nu=\pm 1} (u_{2,m+\mu,n+\nu} + \mu v_{2,m+\mu,n+\nu} + 2^{1/2} \nu w_{2,m+\mu,n+\nu}) - 4u_{1,m,n} + 4u_{3,m,n} \right\}, \quad (6a)$$

$$m_0 \ddot{v}_{1,m,n} = \frac{1}{4}\alpha \left\{ \epsilon_1 [-4v_{1,m,n} + \sum_{\mu,\nu=\pm 1} (-\mu u_{0,m+\mu,n+\nu} + v_{0,m+\mu,n+\nu} + 2^{1/2} \mu \nu w_{0,m+\mu,n+\nu})] - 4v_{1,m,n} + \sum_{\mu,\nu=\pm 1} (\mu u_{2,m+\mu,n+\nu} + v_{2,m+\mu,n+\nu} + 2^{1/2} \mu \nu w_{2,m+\mu,n+\nu}) - 8v_{1,m,n} + 4 \sum_{\mu=\pm 2} v_{1,m+\mu,n} \right\}, \quad (6b)$$

$$m_0 \ddot{w}_{1,m,n} = \frac{1}{4}\alpha \left\{ \epsilon_1 [-8w_{1,m,n} + \sum_{\mu,\nu=\pm 1} (-2^{-1/2} \nu u_{0,m+\mu,n+\nu} + 2^{-1/2} \mu \nu v_{0,m+\mu,n+\nu} + w_{0,m+\mu,n+\nu})] - 8w_{1,m,n} + \sum_{\mu,\nu=\pm 1} (2^{-1/2} \nu u_{2,m+\mu,n+\nu} + 2^{-1/2} \mu \nu v_{2,m+\mu,n+\nu} + w_{2,m+\mu,n+\nu}) \right\}. \quad (6c)$$

For the second layer in from the surface, $l=2$, only the equation for the 1 component of force is different from the bulk. This is

$$m_0 \ddot{u}_{2,m,n} = \frac{1}{4}\alpha \left\{ -8u_{2,m,n} + \sum_{\lambda,\mu,\nu=\pm 1} (u_{l+\lambda,m+\mu,n+\nu} + \lambda \mu v_{l+\lambda,m+\mu,n+\nu} + 2^{1/2} \lambda \nu w_{l+\lambda,m+\mu,n+\nu}) + 4\epsilon_2 (u_{0,m,n} - u_{2,m,n}) + 4(u_{4,m,n} - u_{2,m,n}) \right\}. \quad (7)$$

For reasons of computational convenience, we shall consider crystals with a finite number of layers, so that $0 \leq l \leq N-1$. As was discussed in Ref. 3, the calculation of the mean square displacements involves the inversion of various matrices. For given N , the size of the matrices to be inverted can be reduced by introducing the following symmetry coordinates:

$$u_{l,m,n}(\pm) = \frac{1}{2}\sqrt{2}(u_{l,m,n} \pm u_{N-1-l,m,n}), \quad (8a)$$

$$v_{l,m,n}(\pm) = \frac{1}{2}\sqrt{2}(v_{l,m,n} \pm v_{N-1-l,m,n}), \quad (8b)$$

$$w_{l,m,n}(\pm) = \frac{1}{2}\sqrt{2}(w_{l,m,n} \pm w_{N-1-l,m,n}), \quad (8c)$$

where $0 \leq l \leq (\frac{1}{2}N) - 1$, and N is taken to be an even integer. When one transforms the equations of motion using Eqs. (8), one finds that the variables $u(+)$, $v(-)$, and $w(-)$ are coupled together and that $u(-)$, $v(+)$, and $w(+)$ are coupled together, but that these two sets of variables are decoupled from one another.

It is also advantageous to exploit the translational symmetry parallel to the surfaces by introducing wave vector-components q_1 and q_2 through the transformations

$$u_{l,m,n,i}(\pm) = m_0^{-1/2} [\sum_{\sigma=c,s} T_{\sigma}(q_1, q_2) \xi_{\sigma,l,i}(q_1, q_2, p, \pm)] e^{i\omega_p(q_1, q_2)t}, \quad (9)$$

where i denotes the 1, 2, or 3 direction, p designates the normal modes of frequencies $\omega_p(q_1, q_2)$ corresponding to a given set of values of (q_1, q_2) , $\sigma = c$ or s , and

$$T_c(q_1, q_2) = \cos(mq_1 + nq_2), \quad (10a)$$

$$T_s(q_1, q_2) = \sin(mq_1 + nq_2). \quad (10b)$$

We denote the set of variables $\xi_{\sigma,l,i}(\pm)$, with $l = 0, 1, 2, \dots, (\frac{1}{2}N) - 1$, by $\xi_{\sigma,i}(\pm)$. When Eqs. (9) are substituted into the equations of motion, one finds that the variables $\xi_{\sigma,i}(\pm)$ can be grouped into the following sets of interacting variables: $[\xi_{c,1}(+), \xi_{s,2}(-), \xi_{s,3}(-)]$, $[\xi_{s,1}(+), \xi_{c,2}(-), \xi_{c,3}(-)]$, $[\xi_{c,1}(-), \xi_{s,2}(+), \xi_{s,3}(+)]$, $[\xi_{s,1}(-), \xi_{c,2}(+), \xi_{c,3}(+)]$.

The equations satisfied by $[\xi_{c,1}(+), \xi_{s,2}(-), \xi_{s,3}(-)]$ and $[\xi_{c,1}(-), \xi_{s,2}(+), \xi_{s,3}(+)]$ can be written symbolically as

$$\omega_p^2(q_1, q_2, \pm) \begin{vmatrix} \xi_{c,1}(q_1, q_2, p, \pm) \\ \xi_{s,2}(q_1, q_2, p, \mp) \\ \xi_{s,3}(q_1, q_2, p, \mp) \end{vmatrix} = D_c(q_1, q_2, \pm) \begin{vmatrix} \xi_{c,1}(q_1, q_2, p, \pm) \\ \xi_{s,2}(q_1, q_2, p, \mp) \\ \xi_{s,3}(q_1, q_2, p, \mp) \end{vmatrix} \equiv D_c(q_1, q_2, \pm) \Psi(q_1, q_2, p, \pm), \quad (11)$$

where the $D_c(q_1, q_2, \pm)$ are the reduced dynamical matrices associated with the two sets of variables and are of dimensions $3(\frac{1}{2}N) \times 3(\frac{1}{2}N)$. The form of these matrices is given in the Appendix. Similarly, $[\xi_{s,1}(+), \xi_{c,2}(-), \xi_{c,3}(-)]$ and $[\xi_{s,1}(-), \xi_{c,2}(+), \xi_{c,3}(+)]$ satisfy equations characterized by reduced dynamical matrices $D_s(q_1, q_2, \pm)$. One finds that the diagonal elements of the inverses of $D_s(q_1, q_2, \pm)$ are equal to the corresponding diagonal elements of the inverse of $D_c(q_1, q_2, \pm)$. Using this fact and the methods of Refs. 3, 4 one can write the mean-square-displacement component of atom lmn in the high-temperature limit in the form

$$\langle (u_{lmn})^2 \rangle = (kT/2m_0N^2) \sum_{\tau=\pm} \sum_{q_1, q_2} \times [D_c^{-1}(q_1, q_2, \tau)]_{ii,ii}, \quad (12)$$

where k is Boltzmann's constant, and T is the absolute temperature. An alternative expression for the mean-square-displacement component can be written as^{3,4}

$$\langle (u_{lmn})^2 \rangle = (kT/2m_0N^2) \sum_{\tau=\pm} \sum_{q_1, q_2, p} \times [\Psi_{ii}(q_1, q_2, p, \tau)]^2 / \omega_p^2(q_1, q_2, \tau). \quad (13)$$

In general, our calculations employ Eq. (12); however, Eq. (13) is used for values of the wave-vector

⁴ M. Born, Rept. Progr. Phys. 9, 294 (1942).

components $q_1 = q_2 = \pi$ and $q_1 = q_2 = 2\pi$, which produce a zero eigenvalue. In those cases where no zero eigenvalue occurs, the inverse of $D_c(q_1, q_2, \pm)$ is found numerically using the Gauss-elimination method. We have found that this method gives the diagonal elements of the inverse to six places. The various inverses are then summed over the q values, as indicated in Eq. (12). For the few cases where the inverses of $D_c(q_1, q_2, \pm)$ do not exist, we employ the method of Wilkenson to find the eigenvalues and eigenvectors of $D_c(q_1, q_2, \pm)$. Then Eq. (13) is used, excluding from the sum the term which gives the zero eigenvalue, to find the contribution to the mean square displacements for these q values. In these calculations, at least four significant figures were obtained. This was considered adequate, as the contribution of these two points to the total mean square displacement does not exceed 5%. We also found that the total contribution to the mean-square-displacement components from the sums over $D_c(q_1, q_2, +)$ and $D_c(q_1, q_2, -)$ were identical, thus reducing the calculations by a factor of 2.

III. NUMERICAL RESULTS FOR NICKEL

Calculations of the mean-square-displacement components for atoms in nickel crystals with free surfaces

parallel to the (110) plane have been made. The harmonic approximation with nearest-neighbor central forces and the high-temperature limit have been employed. The force-constants coupling surface atoms to their neighbors are not necessarily assumed to be equal to the bulk-force constant. The value of the bulk-force constant α was chosen to give agreement with the experimental maximum vibrational frequency for unmagnetized nickel obtained by Birgeneau *et al.*⁵ The agreement between calculated dispersion curves and the experimental results³ indicates that this nearest-neighbor model should be reasonably adequate for investigating the lattice-vibrational properties of nickel. The value of α determined by this method is 3.79×10^4 dyn/cm.

In order to find the general effect of changing the three types of force-constants coupling surface atoms to atoms in the interior of the crystal, we varied each of the force constants independently. Figure 2 shows the effect of varying ϵ_1 , with ϵ_2 and ϵ_3 held equal to unity for a crystal with twenty atomic layers. Decreasing ϵ_1 causes all three components of the mean square displacement of atoms on the surface to increase.

TABLE I. Theoretical and experimental mean-square-displacement components at the surface and in the bulk of a face-centered cubic crystal with a (110) free surface.

ϵ_1	ϵ_2	ϵ_3	[110]	$[\bar{1}\bar{1}0]$	[001]	Bulk
1.0	1.0	1.0	0.805	0.643	0.860	0.396
0.5	0.5	1.0	1.331	0.843	1.414	0.404
0.5	0.5	2.2	1.329	0.605	1.413	0.404
Experimental	(Ni)		1.407	0.626	1.407	0.448

In Fig. 3, the effect of varying ϵ_2 , holding ϵ_1 and ϵ_3 equal to unity, is examined for a crystal of twenty atomic layers. As ϵ_2 couples atoms along the [110] direction, decreasing ϵ_2 increases the [110] component of the mean square displacement, as would be expected. The $[\bar{1}\bar{1}0]$ and [001] components are effectively unchanged. Changing ϵ_3 , as shown in Fig. 4, has the same kind of effect on the $[\bar{1}\bar{1}0]$ component, which is increased as ϵ_3 is decreased; the [110] and [001] components are essentially unchanged. Table I gives the experimental values of MacRae in units of kT/α and our previous results for $\epsilon_1 = \epsilon_2 = \epsilon_3 = 1$.

Some interesting effects arise when ϵ_2 is increased above unity while holding ϵ_1 and ϵ_3 equal to unity. Figure 5 shows the dimensionless mean square displacements for this case, with $\epsilon_2 = 2.0$. Note that the component of the mean square displacement in the [110] direction for the surface atom is less than the corresponding value for $\epsilon_2 = 1.0$. This is expected, as the force-constant coupling this atom to an atom two layers removed has been substantially increased. The $[\bar{1}\bar{1}0]$ component of the mean square displacement for

⁵ B. J. Birgeneau, J. Cordes, G. Dolling, and A. B. D. Woods, *Phys. Rev.* **136**, A1359 (1964).

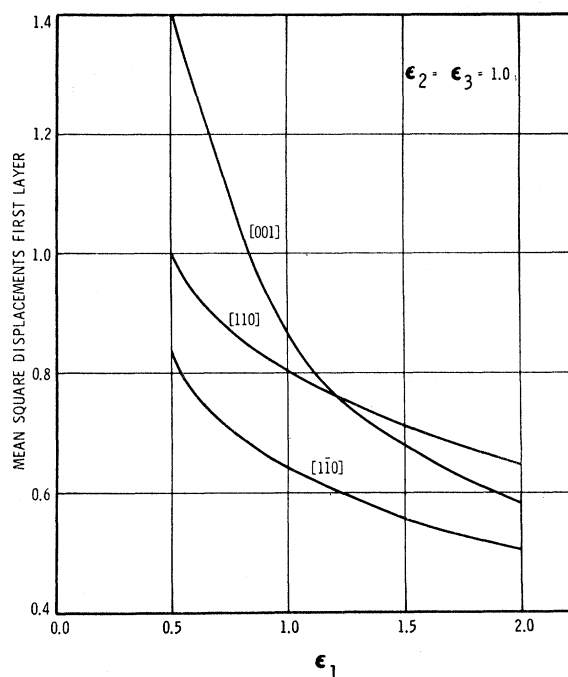


FIG. 2. Components of the mean square displacements of an atom in the first atomic layer in units of kT/α , as a function of ϵ_1 , for $\epsilon_2 = \epsilon_3 = 1$.

the atom in the second layer does not show this effect, as the force-constant coupling this atom to the atom two layers removed has not been altered. We see, in fact, very little difference between these components of the mean square displacement in the first and second layers.

In general, our results show that a mean-square-displacement component is changed significantly only

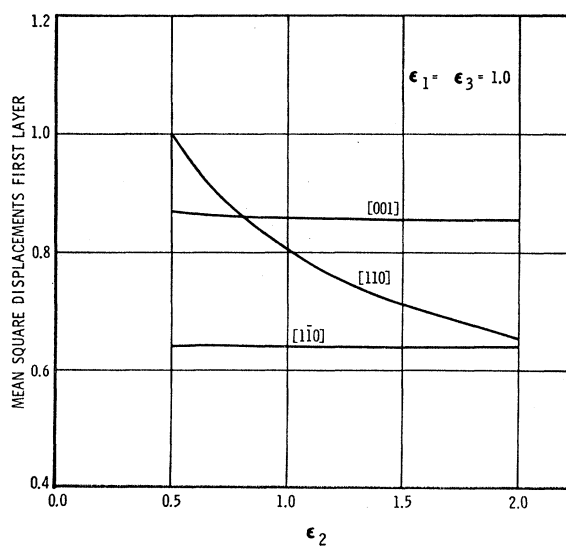


FIG. 3. Components of the mean square displacements of an atom in the first atomic layer in units of kT/α , as a function of ϵ_2 , for $\epsilon_1 = \epsilon_3 = 1$.

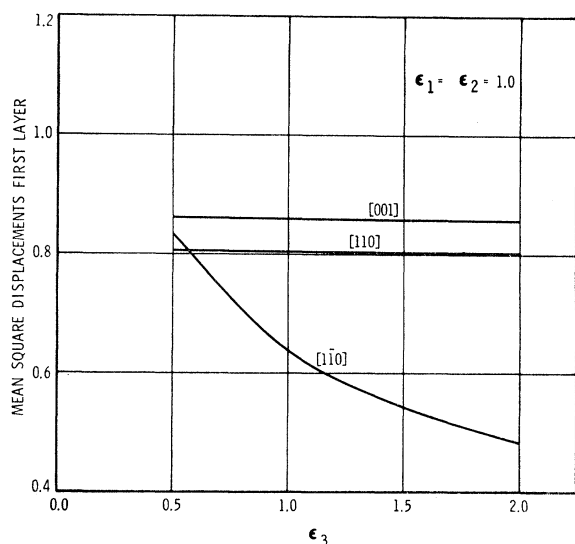


FIG. 4. Components of the mean square displacements of an atom in the first atomic layer in units of kT/α , as a function of ϵ_3 , for $\epsilon_1 = \epsilon_2 = 1$.

if the atom in question is coupled by the force constant which is changed, and only if the line of centers of the coupled atoms is not normal to the displacement direction.

In order to improve the agreement with the experimental data, it is clear that ϵ_1 , ϵ_2 , and ϵ_3 should be changed in such a manner that the $[110]$ and $[001]$ components of the mean square displacements of surface

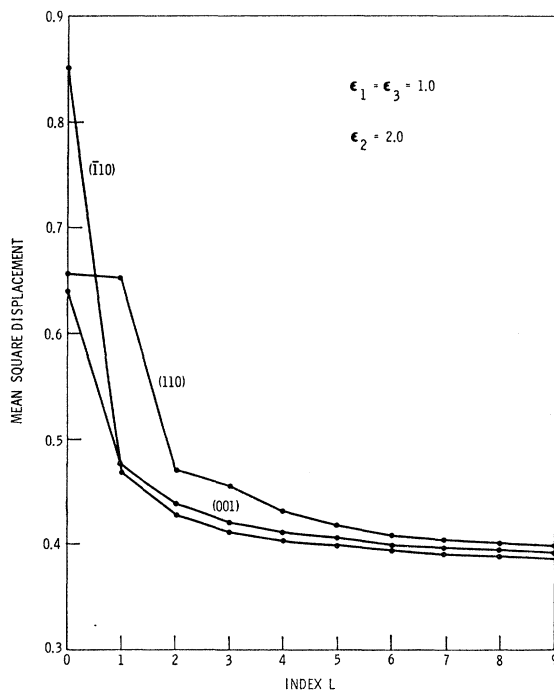


FIG. 5. Components of the mean square displacements as a function of layer index L for $\epsilon_1 = \epsilon_3 = 1.0$, $\epsilon_2 = 2.0$.

atoms are increased while the $[\bar{1}10]$ component is kept roughly the same as in the previous calculations with $\epsilon_3 = 1$. We carried out a series of calculations varying ϵ_1 and ϵ_2 , holding $\epsilon_3 = 1$, and found that $\epsilon_1 = \epsilon_2 = 0.5$ gave the best representation of the data, with $\epsilon_3 = 1$. We then varied ϵ_3 and found that $\epsilon_3 = 2.2$ improved the agreement further. The results of our calculations for a crystal of thirty atomic layers with two free surfaces are shown in Tables I and II. For the case $\epsilon_1 = \epsilon_2 = 0.5$, $\epsilon_3 = 2.2$, the errors are 5.5, 3.7, and 0.4% for the $[110]$, $[\bar{1}10]$, and $[001]$ directions, respectively.

Note that the calculated results for the mean square displacements given in units of kT/α in Tables I and II and Figs. 2-5 are valid for any face-centered cubic lattice with nearest-neighbor forces and surface force constants as indicated, and are not restricted to nickel.

IV. DISCUSSION

The preceding numerical results show that the theoretical mean square displacements can be brought

TABLE II. Mean-square-displacement components in units of kT/α for atoms in successive layers parallel to (110) free surfaces in a crystal thirty layers thick, with $\epsilon_1 = \epsilon_2 = 0.5$, $\epsilon_3 = 2.2$.

Layer number	$[110]$	$[\bar{1}10]$	$[001]$
1	1.329	0.605	1.413
2	0.724	0.525	0.616
3	0.564	0.454	0.467
4	0.488	0.436	0.435
5	0.459	0.426	0.421
6	0.442	0.420	0.415
7	0.431	0.416	0.410
8	0.424	0.412	0.407
9	0.419	0.410	0.405
10	0.415	0.408	0.404
11	0.413	0.406	0.402
12	0.411	0.404	0.402
13	0.409	0.403	0.401
14	0.408	0.403	0.401
15	0.408	0.402	0.400

into reasonable agreement with the experimental data of MacRae by suitable changes in the surface force constants. The question arises whether the magnitude of the changes required is physically reasonable. It would be desirable to answer this question by making fundamental quantum-mechanical calculations of the surface force constants, but at the present time no such calculations appear to be available.

An alternative procedure is to calculate the surface force-constant changes using a postulated interatomic potential such as a Lennard-Jones or Morse potential. The anharmonicity of such potentials leads to changes in the surface force constants from their bulk values. A calculation for the (100) surface of a body-centered cubic lattice has been carried out by Clark *et al.*,⁶ who find decreases in the surface force constants of up to

⁶ B. C. Clark, R. Herman, D. C. Gazis, and R. F. Wallis, in *Proceedings of the Symposium on Ferroelectricity* (Elsevier Publishing Co., Inc., New York, 1967), p. 101.

35%. Recently, Vail has calculated changes in surface force constants for a (100) surface of a simple cubic lattice with Morse-type interactions out to seventh neighbors.⁷ He finds that the nearest-neighbor force constant for vibrations of a surface atom perpendicular to the surface is about 40% smaller than the bulk value, but that for vibrations parallel to the surface, the nearest-neighbor force constant is about 7% larger than the bulk value.

From these considerations, it appears reasonable that ϵ_1 and ϵ_2 should be less than 1.0 and might be as small

as 0.5. The value of 2.2 for ϵ_3 is in the direction indicated by Vail's results, but the amount of deviation from unity must be viewed with some suspicion. In fact, our results for $\epsilon_1 = \epsilon_2 = 0.5$, $\epsilon_3 = 1.0$ are probably in as good agreement with the experimental data as one can reasonably expect, considering the uncertainty in the data and the simplicity of our model.

ACKNOWLEDGMENT

The authors wish to thank Professor J. M. Vail for a report of his work.

APPENDIX

The reduced dynamical matrices $D(q_1, q_2, \pm)$ may be written in terms of the 3×3 matrices d_{ij} as

$$D(q_1, q_2, \pm) = \begin{vmatrix} d_{00}(\pm) & d_{01}(\pm) & d_{02}(\pm) & \cdot & \cdot \\ d_{10}(\pm) & d_{11}(\pm) & d_{12}(\pm) & \cdot & \cdot \\ d_{20}(\pm) & d_{21}(\pm) & d_{22}(\pm) & \cdot & \cdot \\ \vdots & \vdots & \vdots & \vdots & \vdots \\ \cdot & \cdot & \cdot & d_{(N/2)-2, (N/2)-2}(\pm) & d_{(N/2)-2, (N/2)-1}(\pm) \\ \cdot & \cdot & \cdot & d_{(N/2)-1, (N/2)-2}(\pm) & d_{(N/2)-1, (N/2)-1}(\pm) \end{vmatrix}.$$

The matrices d_{ij} are expressed in terms of the quantities $c_1 = \cos q_1$, $c_2 = \cos q_2$, $s_1 = \sin q_1$, and $s_2 = \sin q_2$, and are

$$\begin{aligned} d_{00}(\pm) &= \begin{vmatrix} \epsilon_1 + \epsilon_2 & 0 & 0 \\ 0 & \epsilon_1 + 2\epsilon_3(1 - c_1^2 + s_1^2) & 0 \\ 0 & 0 & 2\epsilon_1 \end{vmatrix}, \\ d_{11}(\pm) &= \begin{vmatrix} 2 + \epsilon_1 & 0 & 0 \\ 0 & 1 + \epsilon_1 + 2(1 - c_1^2 + s_1^2) & 0 \\ 0 & 0 & 2 + 2\epsilon_1 \end{vmatrix}, \\ d_{22}(\pm) &= \begin{vmatrix} 3 + \epsilon_2 & 0 & 0 \\ 0 & 4 - 2(c_1^2 - s_1^2) & 0 \\ 0 & 0 & 4 \end{vmatrix}, \\ d_{ii}(\pm) &= \begin{vmatrix} 4 & 0 & 0 \\ 0 & 4 - 2(c_1^2 - s_1^2) & 0 \\ 0 & 0 & 4 \end{vmatrix}, \quad 3 \leq i \leq (\frac{1}{2}N) - 2 \\ d_{(N/2)-1, (N/2)-1}(\pm) &= \begin{vmatrix} 4 \mp c_1 c_2 & \pm s_1 c_1 & \pm \sqrt{2} c_1 s_2 \\ \pm s_1 c_2 & 4 - 2(c_1^2 - s_1^2) \pm c_1 c_2 & \mp \sqrt{2} s_1 s_2 \\ \pm \sqrt{2} c_1 s_2 & \mp \sqrt{2} s_1 s_2 & 4 \pm 2c_1 c_2 \end{vmatrix}, \\ d_{01}(\pm) &= \epsilon_1 d_{12}(\pm), \\ d_{i, i+1}(\pm) &= \begin{vmatrix} -c_1 c_2 & -s_1 c_2 & -\sqrt{2} c_1 s_2 \\ s_1 c_2 & -c_1 c_2 & \sqrt{2} s_1 s_2 \\ \sqrt{2} c_1 s_2 & \sqrt{2} s_1 s_2 & -2c_1 c_2 \end{vmatrix}, \quad 1 \leq i \leq (\frac{1}{2}N) - 3 \\ d_{10}(\pm) &= \epsilon_1 d_{21}(\pm), \\ d_{i+1, i}(\pm) &= \begin{vmatrix} -c_1 c_2 & s_1 c_2 & \sqrt{2} c_1 s_2 \\ -s_1 c_2 & -c_1 c_2 & \sqrt{2} s_1 s_2 \\ -\sqrt{2} c_1 s_2 & \sqrt{2} s_1 s_2 & -2c_1 c_2 \end{vmatrix}, \quad 1 \leq i \leq (\frac{1}{2}N) - 3 \\ d_{(N/2)-2, (N/2)-1}(\pm) &= \begin{vmatrix} \mp 1 - c_1 c_2 & -s_1 c_2 & -\sqrt{2} c_1 s_2 \\ s_1 c_2 & -c_1 c_2 & \sqrt{2} s_1 s_2 \\ \sqrt{2} c_1 s_2 & \sqrt{2} s_1 s_2 & -2c_1 c_2 \end{vmatrix}, \\ d_{(N/2)-1, (N/2)-2}(\pm) &= \begin{vmatrix} \mp 1 - c_1 c_2 & s_1 c_2 & \sqrt{2} c_1 s_2 \\ -s_1 c_2 & -c_1 c_2 & \sqrt{2} s_1 s_2 \\ -\sqrt{2} c_1 s_2 & \sqrt{2} s_1 s_2 & -2c_1 c_2 \end{vmatrix}, \end{aligned}$$

⁷ J. M. Vail, Bull. Am. Phys. Soc. **12**, 80 (1967); Can. J. Phys. **45**, 2661 (1967).

$$d_{02}(\pm) = \epsilon_2 d_{13}(\pm),$$

$$d_{i,i+2}(\pm) = \begin{vmatrix} -1 & 0 & 0 \\ 0 & 0 & 0 \\ 0 & 0 & 0 \end{vmatrix}, \quad 1 \leq i \leq (\frac{1}{2}N) - 3$$

$$d_{20}(\pm) = \epsilon_2 d_{31}(\pm),$$

$$d_{i+2,i}(\pm) = d_{i,i+2}(\pm), \quad 0 \leq i \leq (\frac{1}{2}N) - 3.$$

PHYSICAL REVIEW

VOLUME 167, NUMBER 3

15 MARCH 1968

Optical Absorption of $\text{Cu}_{1-x-y}\text{Zn}_x\text{Ni}_y$ with $x < 0.25$ and $0.08 < y < 0.10$ at Room Temperature

KLAUS SCHRÖDER AND KARL MAMOLA*

Department of Chemical Engineering and Metallurgy, Syracuse University, Syracuse, New York

(Received 13 October 1967)

The optical absorption of ternary copper-base copper-nickel-zinc alloys with up to 25-at. % zinc and about 10-at. % nickel was determined at room temperature in the wavelength range 260 to 800 nm. The position of the main absorption edge, which for pure copper is observed near 600 nm, moved with increasing zinc concentration to lower wavelength. Within experimental accuracy it was independent of the nickel concentration. This indicates that the extra electrons contributed by Zn atoms do not occupy holes produced by Ni atoms. The secondary absorption structure at 300-nm splits with increasing zinc concentration into two peaks. The peak which moves to higher wavelength is associated with transitions from the Fermi surface to higher bands. It is proposed that the absorption structure which stays at 300 nm independent of the zinc concentration is due to virtual impurity states.

INTRODUCTION

THE electronic structure of alloys is more difficult to determine than the structure of pure metals because the mean free path of electrons is very short. Techniques which are available to determine the Fermi surface of metals frequently cannot be used to study alloys. Therefore, much simpler concepts are used to describe properties of alloys. One of these is the rigid-band model, which states in its simplest form that the properties of alloys depend only on the electron to atom ratio. Investigations on α brass showed that this rigid-band model has to be modified slightly to explain their optical properties.¹ Pure copper exhibits a main absorption edge near 600 nm, and a secondary absorption structure near 300 nm. Alloying copper with zinc shifts the position of the main absorption edge to lower wavelength, and the secondary absorption edge to higher wavelength. This behavior can be interpreted qualitatively using a rigid-band model, if the main absorption edge is associated with interband transitions from the d band to the Fermi surface, and the secondary absorption edge with transitions from the Fermi surface to higher bands. However, the shift of the absorption structures is less than the rigid-band model predicts.

The shift is larger, however, than predicted by Friedel,² who assumed that the extra electron of zinc would form a "cloud" near the zinc nucleus. The rigid-band model fails completely to predict the optical properties of copper-nickel alloys with up to 25-at. % Ni.³ The positions of the main absorption edge and the secondary absorption edge remain within experimental accuracy at 600 nm, or 300 nm, respectively. This result has been explained using the concept of "virtual energy states."^{4,5} These are states which are created below and above the Fermi surface, if nickel atoms replace copper atoms in copper-nickel alloy. The Fermi energy would not change its position in such a model. Experiments on CuNi alloys indicate that nickel impurities create virtual energy states.³

It seemed interesting to measure optical properties of ternary copper-base copper-nickel-zinc alloys $\text{Cu}_{1-x-y}\text{Zn}_x\text{Ni}_y$ to determine if extra electrons from zinc atoms would interact directly with nickel atoms. In that case, the position of the absorption edges would be at the same position as that of an alloy of the composition $\text{Cu}_{1-(x-y)}\text{Zn}_{(x-y)}$. However, if the addition of nickel to

* Present address: Department of Physics, Appalachian State University, Boone, N. C.

¹ M. A. Biondi and J. A. Rayne, *Phys. Rev.* **115**, 1522 (1959).

² J. Friedel, *Proc. Phys. Soc. (London)* **B65**, 769 (1952). *J. Friedel, Ann. Phys.* **9**, 158 (1954). *J. Friedel, Advan. Phys.* **3**, 461 (1964).

³ K. Schröder and D. Öngüt, *Phys. Rev.* **162**, 628 (1967).

⁴ P. de Faget de Casteljau and J. Friedel, *J. Phys. Radium* **17**, 27 (1956).

⁵ P. W. Anderson, *Phys. Rev.* **124**, 41 (1961).